Vessel Plus

Review

Imaging and computational modeling of tricuspid regurgitation and repair

Ashley E. Morgan[1], Kenneth Howell[1], Stacey Chen[2], Rosemarie O. Serrone[1], Yue Zheng[3], Vicky Y. Wang[3], Jiwon J. Kim[4], Eugene Grossi[2], Craig H. Selzman[1], Julius M. Guccione[3], Vikas Sharma[1], Rob MacLeod[5], Mark B. Ratcliffe[3]

[1]Department of Surgery, Cardiothoracic Surgery, University of Utah, Salt Lake City, UT 84112, USA.
[2]Department of Surgery, Cardiothoracic Surgery, New York University School of Medicine, New York, NY 10016, USA.
[3]Department of Bioengineering, Northern California Institute for Research and Education, San Francisco, CA 94121, USA.
[4]Department of Medicine, Cardiology, Weill-Cornell Medical College, New York, NY 10075, USA.
[5]Department of Engineering, University of Utah, Salt Lake City, UT 84112, USA.

Correspondence to: Dr. Ashley E. Morgan, Department of Surgery, Division of Cardiothoracic Surgery, University of Utah, 30 N 1900 E, SOM 3C-127, Salt Lake City, UT 84132, USA. E-mail: ashley-morgan@hsc.utah.edu

Abstract

The tricuspid valve (TV) and right ventricle (RV) are a complex mechanical system. Tricuspid regurgitation impacts a growing and heterogeneous population, leading to right-sided volume overload and right heart failure if left untreated. In part because isolated surgical tricuspid valve repair (TVR) is performed infrequently and has a high mortality, several percutaneous TVR options are being developed. However, the mechanical effects of different types of percutaneous or surgical TVR are unclear. Both the quality of RV imaging and the power of cardiac computational modeling have increased, and accurate computational models of the TV + RV with simulated TVR are now possible. Computational models of TV + RV may aid in patient selection and procedural planning prior to surgical and percutaneous TVR.

Keywords: Adult cardiac surgery, tricuspid regurgitation, bioengineering, computational modeling, finite element modeling

INTRODUCTION

Tricuspid regurgitation (TR) affects an estimated 0.5% of the US adult population, equivalent to the prevalence of aortic stenosis[1]. The population of patients with moderate to severe TR is increasing with

the increasing incidence of atrial fibrillation and with use of mechanical devices such as pacemakers, and it is currently estimated at around 1.6 million Americans[2,3]. Population-based studies have determined that isolated TR in the absence of other cardiac disease is a risk factor for death even when incidentally identified on echocardiography. Further work has shown that, when controlling for other measures of cardiac disease such as depressed left ventricular (LV) ejection fraction and elevated pulmonary artery pressure, moderate to severe TR remains an independent risk factor for both morbidity and mortality[4,5].

Links between TR and increased mortality risk may stem from adverse right ventricle (RV) remodeling. TR provides a nidus for progressive right ventricular dilation, volume overload, and ultimate right heart contractile dysfunction[6]. Supporting this is the finding that increasing severity of TR on imaging is associated with markers of progressive RV dysfunction, such as RV dilation and increased right atrial pressure[4]. The greater the initial burden of TR in untreated patients, the more likely they are to progress over time, and the greater the associated progression of RV dysfunction[7]. Correspondingly, isolated severe TR is associated with increased incidence of heart failure despite maximal medical therapy, a 3-4 × risk of major adverse cardiac events, and a 2-3 × risk of death, after controlling for age and presence of other comorbid conditions[8]. Despite these sobering statistics, ideal management of moderate to severe TR remains unclear.

While surgical valve repair is the standard of care for patients with severe and symptomatic TR, it carries with it a 2-5 × higher risk of mortality than surgery on other cardiac valves, and consequently repair of isolated severe TR is rare[3,9-13]. Furthermore, because of the complex relationship between TR and RV dysfunction, for a subset of patients with a clear indication for surgery, correction of TR results in florid right heart failure, and can be fatal[6]. At present, no predictive index exists to identify such patients preoperatively[14]. Because of the high morbidity and mortality rate of open tricuspid surgery, there is a growing interest in minimally invasive therapies for the tricuspid valve (TV). However, while transcatheter therapies for TR are evolving, they have lagged behind similar interventions for the aortic and mitral valves, and have yet to be incorporated into routine clinical practice[15].

Advances in cardiac imaging have enabled high-resolution assessments of both the RV and TV, providing improved assessment of both structure and function[9,14,16]. Computational models of the RV and TV are underway to accurately represent the mechanical behavior of the right heart under varied conditions[17,18]. The utility of this type of cardiac modeling has been previously demonstrated in the LV and mitral valve, illuminating the effects of surgical procedures such as ring annuloplasty, MitraClip placement, and surgical ventricular restoration[19-22]. Using these techniques to examine the TV will provide insight into the mechanical effects of surgical repair and of novel transcatheter devices, leading to improved care of this large group of patients with diseases of the "forgotten" valve.

RIGHT HEART ANATOMY

The right heart includes the right atrium (RA) and RV, separated by the TV. Deoxygenated venous blood drains from the body into the RA, and is propelled forward into the RV during atrial systole; the TV then acts as a one-way valve preventing regurgitant flow of blood back to the RA during ventricular systole, as blood is ejected from the RV out to the pulmonary circulation to participate in oxygen and carbon dioxide exchange.

TV ANATOMY

The TV is a unique and complex anatomic structure, in a dynamic relationship with the RA and ventricle. The TV is the largest and most apically positioned of the four cardiac valves with a normal orifice area of 7-9 cm^2[23]. The TV complex encompasses valve leaflet, papillary muscles, chordae, and annular components. These components work in a well-coordinated symphony in order for the TV to
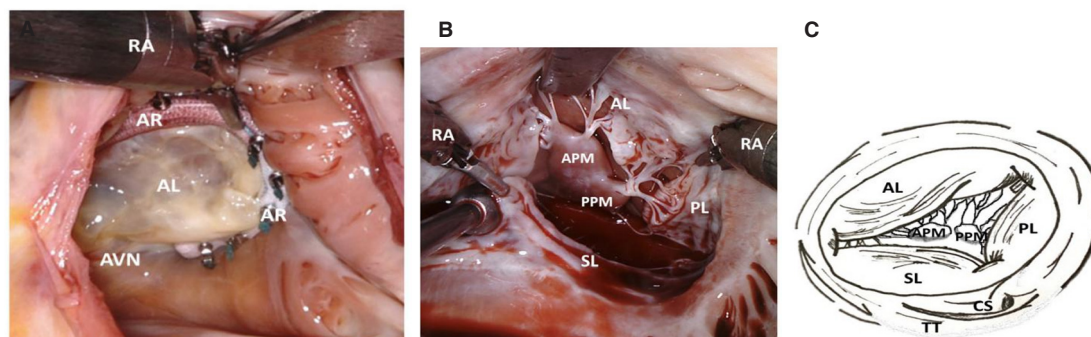
Figure 1. A: Intra-operative photograph of the tricuspid valve with closed leaflets; B: Intra-operative photograph of the tricuspid valve with visible papillary muscles. AL: Anterior leaflet; PL: Posterior leaflet; SL: Septal leaflet; CS: Coronary sinus; TT: Tendon of Todaro; APM: Anterior papillary muscle; PPM: Posterior papillary muscle; RA: Robot arm

physiologically function as a one-way valve. Disorders of the RV or TV disrupt the unidirectional flow of blood, leading to TR.

The TV has three leaflets: anterior, posterior, and septal [Figure 1]. The anterior leaflet is the largest, most mobile, and longest in the radial direction of the three leaflets. The posterior leaflet is the shortest circumferentially and is the least consistently present; in approximately 10% of people, the posterior leaflet and anterior leaflet are fused[24]. The septal leaflet is the least mobile of the three leaflets and is attached to the tricuspid annulus directly above the interventricular septum. These leaflets are suspended in a flexible D-shaped annulus, and tethered to the RV by the sub-valvular apparatus, which is composed of the papillary muscles and their associated chordae tendinae [Figure 1B and C]. The flexible nature of the TV annulus allows it to adapt and change shape during the cardiac cycle, such that it can increase up to 30% in area during end systole/early diastole[23]. There are classically three papillary muscles: the anterior and posterior, which are most reliably present, and the septal papillary muscle, which is absent in approximately 20% of patients[25]. However, the number of papillary muscles is highly variable and can range from two to nine distinct entities. The anterior papillary muscle is the largest, and, in some patients, the moderator band, which carries part of the right bundle branch of the atrioventricular (AV) conduction system, can be found to join the anterior papillary muscle.

The anatomy of adjacent structures is equally important in the operative management of TV disease. There are three important structures to consider: (1) the noncoronary sinus of Valsalva; (2) the conduction system; and (3) the right coronary artery[24]. The noncoronary sinus is located near the commissure between the anterior and septal leaflets of the TV, increasing the risk of aortic perforation with transcatheter devices, which require anchoring in this area. The AV node lies in the apex of the triangle of Koch, and the bundle of His crosses the attachment to the septal leaflet approximately 3-5 mm posterior to the anteroseptal commissure, which can result in heart block if there is excess pressure on the AV node[26]. The right coronary artery originates from the right coronary sinus of Valsalva and courses adjacent to the tricuspid annulus, and it can result in cardiogenic shock secondary to direct injury to the right coronary artery in TV repair[27].

ETIOLOGIES OF TR

TR can be divided into two overarching categories: primary and secondary. Primary TR indicates dysfunction of the valve leaflets or chordae and makes up about 10% of TR in adults[3]. Causes of primary TR include: leaflet damage due to implanted devices, such as pacemakers and catheters; myxomatous valve disease; carcinoid heart syndrome; congenital anomalies of cardiac development; endocarditis; and rheumatic valve disease. In the absence of other cardiac disease, isolated moderate to severe primary TR carries with it an estimated 1.6 × risk of mortality over the general population[1,3].

Secondary TR makes up the remaining 90% of TR in adults and results from right ventricular remodeling in the presence of an otherwise normal TV. Etiologies are diverse and include chronic atrial fibrillation, pulmonary hypertension, left ventricular failure, left to right shunts, right ventricular infarcts, and cardiomyopathies[28]. Secondary TR is associated with papillary muscle displacement, and dilatation and remodeling of the TV annulus, leading to tethering or tenting of the TV leaflets and progressive RV dysfunction.

CLINICAL IMPACT OF TR

It is estimated that about 1.6 million Americans have moderate to severe TR, while only about 8000 will undergo TV surgery annually[3,28]. TV surgery carries a high risk of mortality compared to other cardiac operations: overall in-hospital mortality from isolated TV repair has been reported at around 8.5%, remaining stable over the past decade; this is compared to the 1%-5% mortality expected with isolated repair of any of the other three main cardiac valves[11,12]. This is likely reflective of the late referral of these patients, such that, by the time of surgical evaluation, they often have systemic manifestations of right heart failure (i.e., coagulopathy, hepatic dysfunction, and renal failure). This is in contrast to the paradigm for intervention on left-sided valves, which is to repair or replace before the onset of structural changes to the heart[9].

TIMING AND METHODS OF TRICUSPID INTERVENTION

The 2014 American College of Cardiology/American Heart Association valvular heart disease guidelines strongly recommend isolated TV surgery in severe symptomatic tricuspid stenosis, recommend isolated TV surgery in patients with severe TR who do not respond to medical therapy, and recommend isolated TV surgery in asymptomatic patients with severe TR and at least moderate RV dilation or dysfunction[9]. Despite these recommendations, there remains a large disparity between the number of affected patients and the number surgically repaired[11,12]. It has been suggested that early surgery should be considered in severe TR with RV dilation before the onset of symptoms[6,14]. There are currently no significant published data on an accurate way to assess the TV and RV to determine the potential clinical evolution or recommend the timing of intervention for isolated TR.

Various surgical methods have been applied to repair of the TV, including leaflet augmentation, suture annuloplasty, and the "clover" technique of suturing the center-point of each of the tricuspid leaflets together[29]. The most common method of open surgical repair is ring annuloplasty, whereby a prosthetic, incomplete ring is sutured to the tricuspid annulus to decrease annular size, restore leaflet coaptation, and prevent further annular enlargement [Figure 2A][29]. Because of the high-risk nature of open tricuspid surgery, and the general presence of comorbid conditions among patients with TR, significant interest exists in percutaneous options for tricuspid repair. Methods to deploy the MitraClip (a percutaneous clip designed for mitral valve repair) in the tricuspid position have yielded positive initial results, and work is ongoing to design and test dedicated tricuspid clips and deployment devices [Figure 2B][30].

INCIDENCE OF RV FAILURE AFTER REPAIR AND NEED FOR MECHANICAL RV SUPPORT

The RV is more sensitive to changes in preload and afterload than is the LV[31,32]. RV function can deteriorate in context of alterations in preload or afterload, or direct alterations of RV contractility due to infarction or ischemia. Importantly, acute increases in afterload are especially poorly tolerated by the thin-walled RV. Regardless of surgical or percutaneous repair type, correction of moderate to severe TR results in sudden exposure of the RV to increased afterload when the valve becomes competent. In patients with limited RV reserve, this can result in acute postoperative RV failure, a unique management challenge associated with increased complications and death after tricuspid surgery[33]. The risk of RV dysfunction is higher in the setting of structural remodeling (RV dilation) and/or high pulmonary vascular resistance,
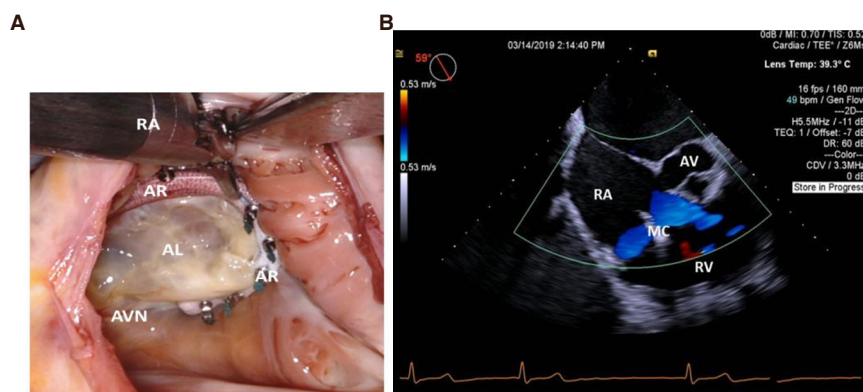
Figure 2. A: Intra-operative photograph of tricuspid annuloplasty ring; B: TEE of MitraCliprepair of the tricuspid. Doppler blood flow on either side of the MitraClip during RV flling is seen in blue. AR: Annuloplasty ring; AL: Anterior leaflet; AVN: AV node; RA: Robot arm; RV: Right ventricle; AV: Aortic Valve; MC: MitraClip

and retrospective studies demonstrate significantly increased mortality and morbidity after TV repair in patients with preexisting reduced right ventricular function[10]. However, there is a paucity of clinical data on the incidence of postoperative RV failure after isolated TV surgery.

Perioperative RV failure can be managed by manipulating preload, afterload, and contractility; however, these efforts may ultimately fail to provide adequate forward flow, leading to a vicious cycle wherein low cardiac output decreases coronary perfusion and further worsens RV function, necessitating initiation of mechanical support for the failing RV[34]. Right ventricular mechanical support methods include percutaneous axial flow pumps such as the Impella RP (Abiomed, Danvers, MA), extracorporeal centrifugal pumps such as the ProtekDuo (LivaNova, London, England), or venoarterial extracorporeal membrane oxygenation (VA-ECMO). However, no predictive model yet exists to identify patients preoperatively who are at high risk of RV failure or who may benefit from preemptive initiation of RV mechanical support.

IMAGING OF THE RV

RV imaging has been traditionally deemed challenging due to its irregular shape (prohibiting geometric assumptions) and thin-walled structure with extensive trabeculations[26,35]. Advances in imaging technology have facilitated higher resolution cardiac assessment, enabling reliable assessment of RV structure, function, and tissue characterizations.

Magnetic resonance imaging

Cardiac magnetic resonance imaging (MRI) is the gold standard for RV imaging, allowing quantification of ventricular volume throughout the cardiac cycle, identification of areas of scar using late gadolinium enhancement, and measurement of global and local RV strain [Figure 3A-C][36]. MRI-based population database studies of thousands of patients have defined normal values for RV mass, volume, and ejection fraction, indexed by age, race, and gender[37]. Cardiac MRI also identifies subtle changes in dysfunctional myocardium, such as non-ischemic fibrosis, which correlate with decreased RV function but are not visible by other imaging modalities[38]. High resolution MRI of *ex-vivo* hearts reveals the complex underlying structure of the RV myocardial fibers, which change angle from the base to the apex of the RV as well as transmurally through the RV wall [Figure 4][39]. Key drawbacks to conventional MRI include significant time for image acquisition, need for operator expertise, cost, closed space imaging environment (in which a patient is supine), and clinical patient stability to tolerate repeated respiratory breath-holds. Furthermore, many implantable cardiac devices are incompatible with MRI scanners, limiting imaging of patient
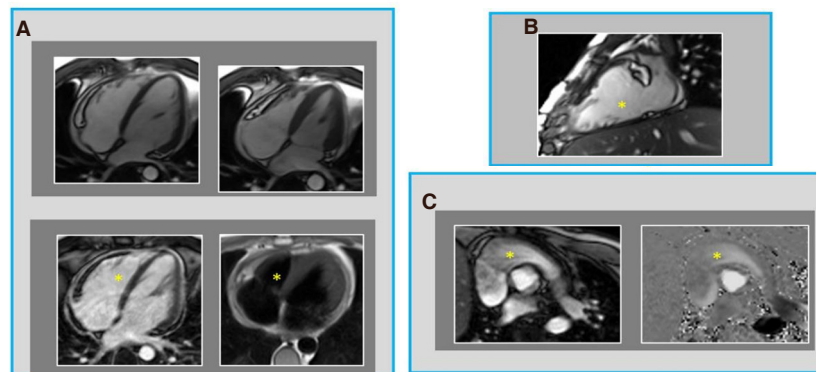
Figure 3. Representative examples of right ventricular assessment via cardiac magnetic resonance (CMR).A: Top: Functional assessment via steady state free precession cine-CMR (left = end-diastole, right = end-systole). Bottom: Myocardial tissue characterization via late gadolinium enhancement CMR (for infarction/fibrosis) and T1-weighted spin echo-CMR (for fat infiltration); B: Dedicated right ventricular functional assessment via cine-CMR; C: Flow assessment via phase-velocity encoded CMR (left = magnitude data, right= phase-encoded data). Asterisk corresponds to the right ventricle in each image
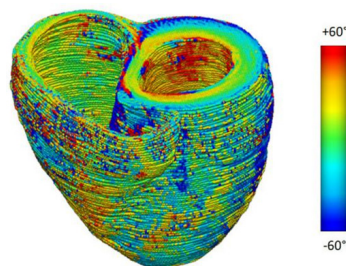

Figure 4. A color map of myofiber helix angles (angles defined with respect to the local circumferential direction) of the LV and RV, derived from an *ex vivo* diffusion tensor MRI of a human heart

populations with pacemakers and implantable defibrillators - patients specifically at high risk for TR and of interest to the current review. While use of MRI conditional devices and free breathing MRI techniques as well as growing expertise in cardiac MRI have bypassed some of these challenges, substantial impediments to widespread utilization persist, highlighting the importance of alternative imaging modalities for RV and TV assessment.

Echocardiography

Transthoracic echocardiography (TTE) is the least invasive and most readily available of all cardiac imaging modalities, and is safe for all patients regardless of clinical condition or presence of implantable devices. To maximize utility of this imaging modality, recent guidelines have been published to standardize RV echocardiography, establishing normal reference values and systematizing the approach to two-dimensional RV imaging[40]. Unfortunately, the RV is retrosternal and visualization may be limited with TTE, depending on patient body habitus. However, general estimates of RV size and function are possible, and correlate well with RV dysfunction identified on MRI[35]. Further information is gained with three-dimensional TTE, allowing quantification of RV ejection fraction (RVEF); depressed RVEF (< 35%-40%) measured by echo has been clinically linked to risk of major adverse cardiac events and cardiac death[33,41]. Structural data from 3D TTE have also been used for RV shape analysis, which is discussed in further detail below. Trans-esophageal echo (TEE) is more invasive and is limited by the anterior position of the TV as compared to the MV, but should be employed when trans-thoracic windows are inadequate for tricuspid visualization[40]. 3D TEE and TTE measures of RV dysfunction provide the closest correlate to RVEF as measured by MRI[35,38].
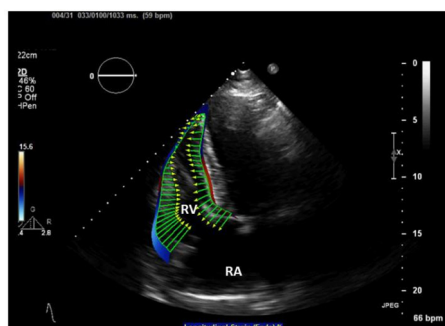
Figure 5. Transthoracic echo with RV speckle tracking based calculation of RV endocardial deformation (green vectors). RA: right atrium; RV: right ventricle

Strain

Myocardial strain is a measurement of relative deformation of a region of myocardium, from a reference state (e.g., end-diastole) to a deformed state (e.g., end-systole). In the context of continuum mechanics, myocardial strain is quantified using a second-order strain tensor given its complex 3D motion[42]. Existing biomechanics and cardiac image analysis often report strains along local wall coordinate system, namely circumferential, longitudinal, and radial directions, because the local wall coordinate system is better aligned with the major mode of deformation of the heart. Global longitudinal strain, especially end-systolic longitudinal strain, is the most commonly used metric in cardiac imaging[43]. For clinical purpose, negative end-systolic longitudinal strain indicates shortening of the LV with respect to end-diastole, with more negative values indicating greater shortening and therefore greater contractility of a region of the heart. Regional Strain can be measured by echocardiography, using techniques such as speckle tracking and tissue Doppler; RV strain measured by 2D echo has been shown to be a stronger predictor of outcomes in patients with heart failure than more conventional measures of cardiac function such as LV ejection fraction and B-type natriuretic peptide [Figure 5][44]. Echo-based RV strain also predicts mortality in heart failure patients listed for cardiac transplantation[45]. As compared to other echocardiographic measures of RV function such as tricuspid annular plane systolic excursion, longitudinal strain measured by echo correlates most strongly with decreased RVEF measured by MRI[38].

Multiple techniques have been developed for MRI-based measures of myocardial strain. Conventional MRI strain measures rely on "tagging", i.e., the encoding of magnetic lines orthogonal to myocardial tissue[46]. The tags are then tracked with post-processing software, yielding fine-detail information on the circumferential, longitudinal, and radial motion of the myocardium. One such MRI technique, known as Displacement ENcoding with Stimulated Echoes (DENSE) MRI, shows promising capability in imaging myocardial displacement on a voxel-by-voxel basis. This technique has been successfully applied to examine LV motion for both human and animals under physiological and pathological conditions[47]. Effort has also recently been made to extend the analysis to the RV in healthy rat hearts[48].

All tag-based techniques require high-resolution MRI and can be limited by the thin wall and trabeculations of the RV, which is often only one to two voxels thick, especially on the free wall. A further limitation is the need for additional time in the MRI scanner for each specialized sequence obtained, which can be a significant factor for patients with TR and heart failure symptoms, with limited ability to lay flat. Feature-tracking is a post-processing solution using standard cine MRI sequences (obtained during every cardiac MRI), applying software that identifies features in an image and tracks them in successive time points, to quantify motion of various regions of the RV[46]. This method has its own limitations, including inability to track motion of less than one-pixel magnitude, and difficulty with out-of-plane motion in 2D images. Both DENSE and feature tracking are evolving tools for detailed analysis of RV function.

IMAGING OF THE TV

Imaging of the right heart, specifically the TV, is imperative to not only understanding TV anatomy and function in each individual to optimize future management, but also to identify the underlying etiology of TR. Thus, evaluation of the structural integrity of the TV leaflets in multiple views with cardiac imaging is critical, as this is the distinguishing feature between primary and secondary TR. With respect to assessing severity of functional TR, special attention should be paid to the tricuspid annulus (TA) size. This can be a challenge, as the tricuspid annulus is a dynamic structure with changing shape and size during respiratory and cardiac cycles, due to the contraction of the surrounding myocardium[49]. Echocardiography is the primary modality used for evaluating the TV[50,51]. The application of 2D TTE to image the TV has several limitations. First, 2D TTE does not provide a complete visualization of the TV; only two TV leaflets can be seen at the same time, while 3D TTE or TEE provides a view of all leaflets simultaneously. Second, 2D TTE underestimates the maximal dimension of the tricuspid annulus compared to 3D TTE or cardiac MRI[52]. This is important to emphasize because there is a growing body of evidence demonstrating the importance of TA diameter as a marker for TV dysfunction, even in the absence of clinically significant TR[53]: normal TA diameter in an adult is 28 ± 5 mm; concomitant TV surgical intervention at the time of left-sided valve surgery is recommended when the TA diameter is ≥ 40 mm[9,54]. Third, 3D TTE provides a more reliable means to identify the TV leaflets and commissures compared to 2D TTE, which is important in evaluating the effect of damage secondary to pacemaker leads or other implanted devices in patients with primary, catheter-related TR[26]. Lastly, in addition to TA diameter, decreased TV leaflet coaptation and degree of leaflet tethering are important prognostic factors predicting outcomes in patients undergoing tricuspid repair[55]. Both of these anatomic pathologies are better visualized using 3D (rather than 2D) TTE.

MODELING TR

Large animal models

Foundational *in-vivo* experiments with sonomicrometry crystals placed in ovine RVs demonstrate that acute RV failure increases RV size, RV free wall strain, and size of the TA with corresponding increase in grade of TR[56,57]. In these large-animal models, tricuspid repair with annuloplasty led to decreased RV size, normalized RV strain, and resolution of TR, supporting tricuspid annuloplasty as a therapy of choice for TR, with potential to improve RV function[56]. Such animal models provide valuable insights into the origins of RV failure and choice of intervention; however, they are invasive, cumbersome, and by nature cannot be replicated in humans. Development of non-invasive techniques to reproduce these results is consequently an important clinical target.

Computational models of the RV, LV, and TV

With the above advances in cardiac imaging, it is possible to accurately define RV structure, including fiber angles, shape, and areas of ischemia and fibrosis; RV function, including strain in varying regions; TV structure, function, and pathology; and the geometric and functional relationships among the RV, LV, and TV. Using these imaging modalities, an important clinical target is development of accurate computational models of the LV, RV, and TV. Such models will help predict the mechanical effects of tricuspid repair and identify patients at risk of RV dysfunction after such repair. The following efforts are underway in model development.

Shape analysis

Cardiac shape is intimately related to function and provides visual evidence of the pathological changes of cardiac disease. This has been demonstrated most extensively in the LV, where remodeling towards a spherical shape correlates with decreased exercise tolerance and increased mortality[58]. However, as discussed above, the shape of the RV is not simple to describe, and more nuanced methods are required. One such method is statistical shape analysis, a mathematical tool allowing non-invasive identification of

patterns of cardiac structure, which can then be related to function and correlated with clinical outcomes. This has been previously used on the RV to identify differences in patients with pulmonary hypertension (PH) compared to normal controls, demonstrating that patients with PH have increased RV eccentricity (a rounder shape), with bulging of the apex and the tricuspid annulus[59]. Increased RV size and sphericity have also been associated with the known cardiovascular risk factors of hypertension, diabetes, obesity, and smoking[60]. In congenital heart disease, for patients with single-ventricle pathology, changes in ventricular shape have been clinically correlated to symptom severity[58]. As data accrue for different RV and TV pathologies, shape analysis will allow creation of non-invasive predictive tools of disease severity and outcomes.

Finite element modeling
Finite element (FE) modeling is a tool that allows the calculation of the stress-strain behavior of complex materials by breaking them down into small pieces, or elements. This tool has been applied for the last three decades to increase understanding of cardiac mechanics in diverse ways, including modeling the LV and mitral valve and simulating mitral ring annuloplasty, mitral leaflet resection, and percutaneous mitral clip application[19-22,61]. Modeling of the TV has lagged behind models of the left heart; the RV and TV are more complex in shape and behavior than the LV and mitral valve; their anatomy is more variable between patients and between time points in the same patient; the right and left heart are interdependent, with RV behavior altered by LV pressure and by the function of the interventricular septum; and, to model the right heart, some measures of right-sided cavity pressures are required, which typically involve invasive procedures such as cardiac catheterization. Furthermore, extant computational models ignore the complex interaction between the TV and RV, and as yet, no patient-specific models of the RV + TV, or the LV + RV + TV, have been created. Development of such models will allow direct comparison of different repairs for a specific patient to determine the ideal repair type, accounting for the effect of such repairs on the ventricles and valve as a unit.

Modeling the RV + LV
To create an FE model of the myocardium, the 3D geometry of the ventricles is first captured with cardiac imaging, using echo, computed tomography (CT), or cardiac MRI. These images are "contoured", outlining the endocardium and epicardium, to create a virtual mesh of the LV, RV, or both. The stress-strain relationships, or material property laws, of regions of the myocardium are then specified. Multiple formulations of these material property laws exist; our lab employs the version developed by Drs. McCulloch and Guccione (CMISS/Continuity)[62]. These laws are based directly on the 3D fiber angle distributions of the myocardium [Figure 4], are commonly used, and have been validated experimentally under multiple conditions[63,64]. Biventricular models of rat, swine, and canine hearts have been created with this technique to demonstrate increased myocardial stress in heart failure and pressure overload[65-67]. In addition, of more direct clinical relevance, human, patient-specific biventricular models have been created to accurately predict the effect of cardiac resynchronization therapy[68]. To date, these models have not examined the ventricles in patients with TR, and they have not incorporated the TV.

Modeling the isolated TV
To create patient-specific models of the TV, high-resolution images are required to describe its complex valvular geometry. Initial studies focused on excised cadaver valves, which are stationary and easy to structurally define[69]. In living patients, 3D echocardiography images of the TV can be contoured in individual slices at a particular point in the cardiac cycle, to obtain a mesh of the overall valvular structure. Material properties are then applied as described above for the myocardium; these properties have been obtained experimentally from excised leaflet tissue, using predominantly biaxial stretching to determine stress-strain relationships[70]. Using these techniques, the first computational model of the TV, based on excised human cadaver tissue, was created in 2010[69]. Initial patient-specific models of the
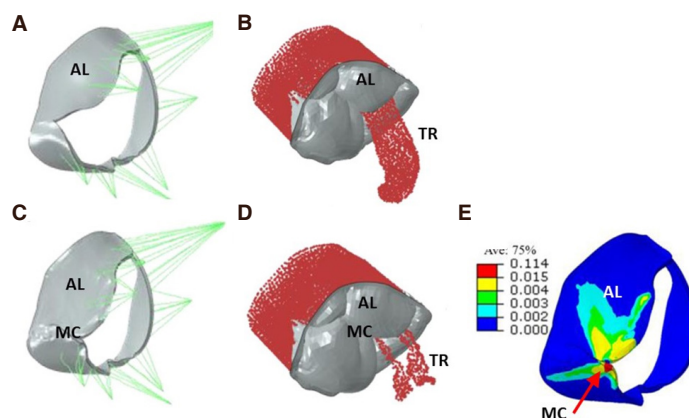
Figure 6. FE model with simulated tricuspid regurgitation (TR) before and after virtual MitraClip (MC). A: baseline mode; B: with TR jet; C: model after virtual MC; D: showing a reduced amount of TR and E) leaflet stress after virtual MC. AL: Anterior leaflet

isolated TV in healthy subjects have established normal values for stress and strain in the valve leaflets and chordae[18,49]; the first foray into modeling TV pathology modeled the geometry of intact and prolapsing valve leaflets based on multi-slice CT images[71]; and the first simulated tricuspid repair incorporated fluid-structure interaction models of MitraClip application to a regurgitant TV, demonstrating the utility of percutaneous therapy as an addition to the limited armamentarium of TR treatments [Figure 6][17]. The details of fluid-structure interaction are beyond the scope of this review; however, incorporating the specifics of regurgitant volumes, as well as the number and direction of regurgitant jets, does allow further accuracy in modeling, providing finer details of the effect of specific valvular repair techniques. Currently, no computational model of the TV includes the RV or LV, limiting investigations into functional TR.

Future directions: modeling the TV + RV + LV
Creating a patient-specific model of the TV + RV + LV is within the current bounds of computational and imaging possibility. This model will allow description of such pathologies as TR secondary to LV failure and prediction of RV dysfunction after tricuspid repair. The addition of the ventricles into models of TR will also delineate the ventricular effects of percutaneous tricuspid interventions, as well as tricuspid repair; because abnormal ventricular strain predicts adverse ventricular remodeling and repair failure over time, including the ventricles into mechanical models of tricuspid disease is a key component of predicting the long-term effects of tricuspid interventions. As statistical shape analysis techniques identify key changes in RV and LV geometry by varying etiologies of tricuspid disease, patients may be classified by non-invasive imaging into groups according to disease severity and type of ventricular derangement; with FE modeling techniques, the understanding of tricuspid interventions can move beyond patient specific modeling to generalized applications based on these imaging characteristics[58].

CONCLUSION

With advances in cardiac imaging come new insights into the importance of the RV and TV in cardiovascular disease. TR remains an under-treated entity, and surgical tricuspid repair carries a high mortality rate. Computational modeling of the TV, RV, and LV based on high-resolution cardiac MRI and echocardiography allow creation of non-invasive patient-specific models of tricuspid repair, helping to solve several vexing clinical problems. First, right heart failure after cardiac surgery requires complex supportive care and carries with it a high mortality rate; no models yet exist to accurately predict or deter this outcome. A combination of statistical shape methods and FE models of the right heart may help identify at-risk RVs, allowing for better preoperative patient selection, and identification of patients who may need prophylactic right-sided mechanical circulatory support at the time of valve repair. Second, open

cardiac surgery is not a practical option for many patients with TR, due to the prevalence of comorbid conditions; computational modeling allows development and testing of novel devices for percutaneous repair, potentially reaching a greater population of patients with TR. Third, and beyond the scope of this review, the realm of congenital cardiac surgery involves treatment of patients with a broad spectrum of valvular and ventricular disease; the opportunity to model such repairs in-silico prior to operating on an individual patient provides for customization of patient-specific repair types with deeper understanding of their immediate and long-term mechanical effects.

DECLARATIONS

Authors' contributions
Primary author, manuscript design, preparation, editing: Morgan AE
Author of the section "Clinical Impact of TR": Howell K
Contributed to the tricuspid anatomy and background sections: Chen S
Figure designs and original drawings: Serrone RO
Contributed to cardiac imaging and computational modeling sections: Zheng Y
Contributed to cardiac imaging and computation modeling sections, figures: Wang VY
Contributed to echocardiography and imaging sections: Kim JJ
Contributed to anatomy and background sections, intraoperative images: Grossi E
Surgical approach and future directions: Selzman CH
Contributed to modeling section: Guccione JM
Surgical approach and future directions: Sharma V
Modeling and future directions: MacLeod R
Senior author, oversight, editing, figure: Ratcliffe MB

Availability of data and materials
Not applicable.

Financial support and sponsorship
None.

Conflicts of interest
All authors declared that there are no conflicts of interest.

Ethical approval and consent to participate
Not applicable.

Consent for publication
Not applicable.

Copyright

REFERENCES

1. Topilsky Y, Maltais S, Medina Inojosa J, Oguz D, Michelena H, et al. Burden of tricuspid regurgitation in patients diagnosed in the community setting. JACC Cardiovasc Imaging 2019;12:433-42.
2. Singh JP, Evans JC, Levy D, Larson MG, Freed LA, et al. Prevalence and clinical determinants of mitral, tricuspid, and aortic regurgitation (the framingham heart study). Am J Cardiol 1999;83:897-902.
3. Fender EA, Zack CJ, Nishimura RA. Isolated tricuspid regurgitation: outcomes and therapeutic interventions. Heart 2018;104:798-806.
4. Nath J, Foster E, Heidenreich PA, Heidenreich PA. Impact of tricuspid regurgitation on long-term survival. J Am Coll Cardiol 2004;43:405-9.

5. Fender EA, Petrescu I, Ionescu F, Zack CJ, Pislaru SV, et al. Prognostic importance and predictors of survival in isolated tricuspid regurgitation: a growing problem. Mayo Clin Proc 2019;94:2032-9.
6. Taramasso M, Gavazzoni M, Pozzoli A, Dreyfus GD, Bolling SF, et al. Tricuspid regurgitation: Predicting the need for intervention, procedural success, and recurrence of disease. JACC Cardiovasc Imaging 2019;12:605-21.
7. Goldstone AB, Howard JL, Cohen JE, MacArthur JW, Atluri P, et al. Natural history of coexistent tricuspid regurgitation in patients with degenerative mitral valve disease: Implications for future guidelines. J Thorac Cardiovasc Surg 2014;148:2802-9.
8. Topilsky Y, Nkomo VT, Vatury O, Michelena HI, Letourneau T, et al. Clinical outcome of isolated tricuspid regurgitation. JACC Cardiovasc Imaging 2014;7:1185-94.
9. Nishimura RA, Otto CM, Bonow RO, Carabello BA, Erwin JP, et al. 2014 AHA/ACC guideline for the management of patients with valvular heart disease: a report of the american college of cardiology/american heart association task force on practice guidelines. J Thorac Cardiovasc Surg 2014;148:e1-132.
10. Subbotina I, Girdauskas E, Bernhardt AM, Sinning C, et.al. Comparison of outcomes of tricuspid valve surgery in patients with reduced and normal right ventricular function. Thorac Cardiovasc Surg 2017;65:617-25.
11. Dhoble A, Zhao Y, Vejpongsa P, Loghin C, Smalling RW, et al. National 10-year trends and outcomes of isolated and concomitant tricuspid valve surgery. J Cardiovasc Surg (Torino) 2019;60:119-27.
12. Zack CJ, Fender EA, Chandrashekar P, Reddy YNV, Bennett CE, et al. National trends and outcomes in isolated tricuspid valve surgery. J Am Coll Cardiol 2017;70:2953-60.
13. LaPar DJ, Likosky DS, Zhang M, Theurer P, Fonner CE, et al. Development of a risk prediction model and clinical risk score for isolated tricuspid valve surgery. Ann Thorac Surg 2018;106:129-36.
14. Rana B, Robinson S, Francis R, Toshner M, Swaans MJ, et al. Tricuspid regurgitation and the right ventricle: Risk stratification and timing of intervention. Echo Res Pract 2019;6:R25-39.
15. Demir OM, Regazzoli D, Mangieri A, Ancona MB, Mitomo S, et al. Transcatheter tricuspid valve replacement: principles and design. Front Cardiovasc Med 2018;5:129.
16. Partington SL, Kilner PJ. How to image the dilated right ventricle. Circ Cardiovasc Imaging 2017;10.
17. Dabiri Y, Yao J, Sack KL, Kassab GS, Guccione JM. Tricuspid valve regurgitation decreases after mitraclip implantation: Fluid structure interaction simulation. Mech Res Commun 2019;97:96-100.
18. Kong F, Pham T, Martin C, McKay R, Primiano C, et al. Finite element analysis of tricuspid valve deformation from multi-slice computed tomography images. Ann Biomed Eng 2018;46:1112-27.
19. Morgan AE, Pantoja JL, Weinsaft J, Grossi E, Guccione JM, et al. Finite element modeling of mitral valve repair. J Biomech Eng 2016;138:021009.
20. Morgan AE, Pantoja JL, Grossi EA, Ge L, Weinsaft JW, et al. Neochord placement versus triangular resection in mitral valve repair: a finite element model. J Surg Res 2016;206:98-105.
21. Pantoja JL, Zhang Z, Tartibi M, Sun K, Macmillan W, et al. Residual stress impairs pump function after surgical ventricular remodeling: a finite element analysis. Ann Thorac Surg 2015;100:2198-205.
22. Pantoja JL, Morgan AE, Grossi EA, Jensen MO, Weinsaft JW, et al. Undersized mitral annuloplasty increases strain in the proximal lateral left ventricular wall. Ann Thorac Surg 2017;103:820-7.
23. Hahn RT. State-of-the-art review of echocardiographic imaging in the evaluation and treatment of functional tricuspid regurgitation. Circ Cardiovas Imaging 2016;9.
24. Dahou A, Levin D, Reisman M, Hahn RT. Anatomy and physiology of the tricuspid valve. JACC Cardiovasc Imaging 2019;12:458-68.
25. Tretter JT, Sarwark AE, Anderson RH, Spicer DE. Assessment of the anatomical variation to be found in the normal tricuspid valve. Clin Anat 2016;29:399-407.
26. Khalique OK, Cavalcante JL, Shah D, Guta AC, ZhanY, et al. Multimodality imaging of the tricuspid valve and right heart anatomy. JACC Cardiovasc Imaging 2019;12:516-31.
27. Diez-Villanueva P, Gutierrez-Ibanes E, Cuerpo-Caballero GP, Sanz-Ruiz R, Abeytua M, et al. Direct injury to right coronary artery in patients undergoing tricuspid annuloplasty. Ann Thoracic Surg 2014;97:1300-5.
28. Taramasso M, Vanermen H, Maisano F, Guidotti A, La Canna G, et al. The growing clinical importance of secondary tricuspid regurgitation. J Am Coll Cardiol 2012;59:703-10.
29. Belluschi I, Del Forno B, Lapenna E, Nisi T, Iaci G, et al. Surgical techniques for tricuspid valve disease. Front Cardiovasc Med 2018;5:118.
30. Tang GHL. Tricuspid clip: step-by-step and clinical data. Interv Cardiol Clin 2018;7:37-45.
31. Reuse C, Vincent JL, Pinsky MR. Measurements of right ventricular volumes during fluid challenge. Chest 1990;98:1450-4.
32. MacNee W. Pathophysiology of cor pulmonale in chronic obstructive pulmonary disease. Part one. Am J Respir Crit Care Med 1994;150:833-52.
33. Park K, Kim HK, Kim YJ, Cho GY, Kim KH, et al. Incremental prognostic value of early postoperative right ventricular systolic function in patients undergoing surgery for isolated severe tricuspid regurgitation. Heart 2011;97:1319-25.
34. Estrada VHN, Franco DLM, Moreno AAV, Gambasica JAR, Nunez CCC. Postoperative right ventricular failure in cardiac surgery. Cardiol Res 2016;7:185-95.
35. Abouzeid CM, Shah T, Johri A, Weinsaft JW, Kim J. Multimodality imaging of the right ventricle. Curr Treat Options Cardiovasc Med 2017;19:82.

36. Marcu CB, Beek AM, Van Rossum AC. Cardiovascular magnetic resonance imaging for the assessment of right heart involvement in cardiac and pulmonary disease. Heart Lung Circ 2006;15:362-70.

37. Kawut SM, Lima JA, Barr RG, Chahal H, Jain A, et al. Sex and race differences in right ventricular structure and function: the multi-ethnic study of atherosclerosis-right ventricle study. Circulation 2011;123:2542-51.

38. Di Franco A, Kim J, Rodriguez-Diego S, Khalique O, Siden JY, et al. Multiplanar strain quantification for assessment of right ventricular dysfunction and non-ischemic fibrosis among patients with ischemic mitral regurgitation. PloS One 2017;12:e0185657.

39. Helm PA, Tseng HJ, Younes L, McVeigh ER, Winslow RL. Ex vivo 3D diffusion tensor imaging and quantification of cardiac laminar structure. Magn Reson Med 2005;54:850-9.

40. Rudski LG, Lai WW, Afilalo J, Hua L, Handschumacher MD, et al. Guidelines for the echocardiographic assessment of the right heart in adults: a report from the american society of echocardiography endorsed by the european association of echocardiography, a registered branch of the european society of cardiology, and the canadian society of echocardiography. J Am Soc Echocardiogr 2010;23:685-713.

41. Nagata Y, Wu VC, Kado Y, Otani K, Lin FC, et al. Prognostic value of right ventricular ejection fraction assessed by transthoracic 3D echocardiography. Circ Cardiovasc Imaging 2017;10.

42. Smiseth OA, Torp H, Opdahl A, Haugaa KH, Urheim S. Myocardial strain imaging: how useful is it in clinical decision making? Eur Heart J 2016;37:1196-207.

43. Voigt JU, Pedrizzetti G, Lysyansky P, Marwick TH, Houle H, et al. Definitions for a common standard for 2D speckle tracking echocardiography: consensus document of the EACVI/ASE/industry task force to standardize deformation imaging. Eur Heart J Cardiovasc Imaging 2015;16:1-11.

44. Iacoviello M, Citarelli G, Antoncecchi V, Romito R, Monitillo F, et al. Right ventricular longitudinal strain measures independently predict chronic heart failure mortality. Echocardiography 2016;33:992-1000.

45. Cameli M, Righini FM, Lisi M, Bennati E, Navarri R, et al. Comparison of right versus left ventricular strain analysis as a predictor of outcome in patients with systolic heart failure referred for heart transplantation. Am J Cardiol 2013;112:1778-84.

46. Scatteia A, Baritussio A, Bucciarelli-Ducci C. Strain imaging using cardiac magnetic resonance. Heart Fail Rev 2017;22:465-76.

47. Haggerty CM, Kramer SP, Binkley CM, Powell DK, Mattingly AC, et al. Reproducibility of cine displacement encoding with stimulated echoes (dense) cardiovascular magnetic resonance for measuring left ventricular strains, torsion, and synchrony in mice. J Cardiovasc Magn Reson 2013;15:71.

48. Liu ZQ, Zhang X, Wenk JF. Quantification of regional right ventricular strain in healthy rats using 3D spiral cine dense MRI. J Biomech 2019;94:219-223.

49. Fukuda S, Saracino G, Matsumura Y, Daimon M, Tran H, et al. Three-dimensional geometry of the tricuspid annulus in healthy subjects and in patients with functional tricuspid regurgitation: a real-time, 3-dimensional echocardiographic study. Circulation 2006;114:I492-8.

50. Anwar AM, Geleijnse ML, Soliman OI, McGhie JS, Frowijn R, et al. Assessment of normal tricuspid valve anatomy in adults by real-time three-dimensional echocardiography. Int J Cardiovasc Imaging 2007;23:717-24.

51. Dreyfus J, Durand-Viel G, Raffoul R, Alkhoder S, Hvass U. Comparison of 2-dimensional, 3-dimensional, and surgical measurements of the tricuspid annulus size: clinical implications. Circ Cardiovasc Imaging 2015;8:e003241.

52. Huttin O, Voilliot D, Mandry D, Venner C, Juilliere Y, et al. All you need to know about the tricuspid valve: tricuspid valve imaging and tricuspid regurgitation analysis. Arch Cardiovasc Dis 2016;109:67-80.

53. Dreyfus GD, Corbi PJ, Chan KM, Bahrami T. Secondary tricuspid regurgitation or dilatation: which should be the criteria for surgical repair? Ann Thorac Surg 2005;79:127-32.

54. Antunes MJ, Rodriguez-Palomares J, Prendergast B, Bonis MD, Rosenhek R, et al. Management of tricuspid valve regurgitation: Position statement of the european society of cardiology working groups of cardiovascular surgery and valvular heart disease. Eur J Cardiothoracic Surg 2017;52:1022-30.

55. Chen Y, Liu YX, Yu YJ, Wu MZ, Lam YM, et al. Prognostic value of tricuspid valve geometry and leaflet coaptation status in patients undergoing tricuspid annuloplasty: a three-dimensional echocardiography study. J Am Soc Echocardiogr 2019;32:1516-25.

56. Jazwiec T, Malinowski M, Bush J, Goehler M, Quay N, et al. Right ventricular free wall stress after tricuspid valve annuloplasty in acute ovine right heart failure. J Thoracic Cardiovas Surg 2019;158:759-68.

57. Malinowski M, Proudfoot AG, Eberhart L, Schubert H, Wodarek J, et al. Large animal model of acute right ventricular failure with functional tricuspid regurgitation. Int J Cardiol 2018;264:124-9.

58. Farrar G, Suinesiaputra A, Gilbert K, Perry JC, Hegde S, et al. Atlas-based ventricular shape analysis for understanding congenital heart disease. Prog Pediatr Cardiol 2016;43:61-9.

59. Leary PJ, Kurtz CE, Hough CL, Waiss MP, Ralph DD, et al. Three-dimensional analysis of right ventricular shape and function in pulmonary hypertension. Pulm Circ 2012;2:34-40.

60. Mauger C, Gilbert K, Lee AM, Sanghvi MM, Aung N, et al. Right ventricular shape and function: cardiovascular magnetic resonance reference morphology and biventricular risk factor morphometrics in uk biobank. J Cardiovasc Magn Reson 2019;21:41.

61. Morgan AE, Wozniak CJ, Gulati S, Ge L, Grossi EA, et al. Association of uneven mitraclip application and leaflet stress in a finite element model. JAMA Surg 2017;152:111-4.

62. Guccione JM, McCulloch AD, Waldman LK. Passive material properties of intact ventricular myocardium determined from a cylindrical model. J Biomech Eng 1991;113:42-55.

63. Guccione JM, Waldman LK, McCulloch AD. Mechanics of active contraction in cardiac muscle: Part ii--cylindrical models of the systolic left ventricle. J Biomech Eng 1993;115:82-90.

64. Guccione JM, McCulloch AD. Mechanics of active contraction in cardiac muscle: Part i--constitutive relations for fiber stress that describe deactivation. J Biomech Eng 1993;115:72-81.

65. Wenk JF, Ge L, Zhang Z, Soleimani M, Potter DD, et al. A coupled biventricular finite element and lumped-parameter circulatory system model of heart failure. Comput Methods Biomech Biomed Engin 2013;16:807-18.

66. Masithulela F. Bi-ventricular finite element model of right ventricle overload in the healthy rat heart. Biomed Mater Eng 2016;27:507-25.

67. Sack KL, Aliotta E, Ennis DB, Choy JS, Kassab GS, et al. Construction and validation of subject-specific biventricular finite-element models of healthy and failing swine hearts from high-resolution dt-mri. Front Physiol 2018;9:539.

68. Okada JI, Washio T, Nakagawa M, Watanabe M, Kadooka Y, et al. Multi-scale, tailor-made heart simulation can predict the effect of cardiac resynchronization therapy. J Mol Cell Cardiol 2017;108:17-23.

69. Stevanella M, Votta E, Lemma M, Antona C, Redaelli A. Finite element modelling of the tricuspid valve: a preliminary study. Med Eng Phys 2010;32:1213-23.

70. Lee CH, Laurence DW, Ross CJ, Kramer KE, Babu AR, et al. Mechanics of the tricuspid valve-from clinical diagnosis/treatment, in-vivo and in-vitro investigations, to patient-specific biomechanical modeling. Bioengineering (Basel) 2019;6:47.

71. Kamensky D, Xu F, Lee CH, Yan J, Bazilevs Y, et al. A contact formulation based on a volumetric potential: application to isogeometric simulations of atrioventricular valves. Comput Methods Appl Mech Eng 2018;330:522-46.